The Compact Muon Solenoid Experiment

Conference Report

P-stop isolation study of irradiated n-in-p type silicon strip sensors for harsh radiation environment

Martin Printz for the CMS Collaboration

Abstract

In order to determine the most radiation hard silicon sensors for the CMS Experiment after the Phase II Upgrade in 2023 a comprehensive study of silicon sensors after a fluence of up to $1.5 \times 10^{15}\ n_{eq}/cm^2$ corresponding to 3000 fb^{-1} after the HL-LHC era has been carried out. The results led to the decision that the future Outer Tracker (20 cm$<R<$110 cm) of CMS will consist of n-in-p type sensors. This technology is more radiation hard but also the manufacturing is more challenging compared to p-in-n type sensors due to additional process steps in order to suppress the accumulation of electrons between the readout strips. One possible isolation technique of adjacent strips is the p-stop structure which is a p-type material implantation with a certain pattern for each individual strip. However, electrical breakdown and charge collection studies indicate that the process parameters of the p-stop structure have to be carefully calibrated in order to achieve a sufficient strip isolation but simultaneously high breakdown voltages. Therefore a study of the isolation characteristics with four different silicon sensor manufacturers has been executed in order to determine the most suitable p-stop parameters for the harsh radiation environment during HL-LHC. Several p-stop doping concentrations, doping depths and different p-stop pattern have been realized and experiments before and after irradiation with protons and neutrons have been performed and compared to T-CAD simulation studies with Synopsys Sentaurus. The measurements combine the electrical characteristics measured with a semi-automatic probestation with Sr90 signal measurements and analogue readout. Furthermore, some samples have been investigated with the help of a cosmic telescope with high resolution allowing charge collection studies of MIPs penetrating the sensor between two strips.

Presented at *10th Hiroshima 10th International Hiroshima Symposium on the Development and Application of Semiconductor Tracking Detectors, Xian, China*

P-stop isolation study of irradiated n-in-p type silicon strip sensors for harsh radiation environment

Martin Printz on behalf of the CMS Tracker Collaboration

Institut fuer Experimentelle Kernphysik, KIT

Abstract

In order to determine the most radiation hard silicon sensors for the CMS Experiment after the Phase II Upgrade in 2023 a comprehensive study of silicon sensors after a fluence of up to 1.5×10^{15} n_{eq}/cm^2 corresponding to 3000 fb^{-1} after the HL-LHC era has been carried out. The results led to the decision that the future Outer Tracker (20 cm<R<110 cm) of CMS will consist of n-in-p type sensors. This technology is more radiation hard but also the manufacturing is more challenging compared to p-in-n type sensors due to additional process steps in order to suppress the accumulation of electrons between the readout strips. One possible isolation technique of adjacent strips is the p-stop structure which is a p-type material implantation with a certain pattern for each individual strip. However, electrical breakdown and charge collection studies indicate that the process parameters of the p-stop structure have to be carefully calibrated in order to achieve a sufficient strip isolation but simultaneously high breakdown voltages. Therefore a study of the isolation characteristics with four different silicon sensor manufacturers has been executed in order to determine the most suitable p-stop parameters for the harsh radiation environment during HL-LHC. Several p-stop doping concentrations, doping depths and different p-stop pattern have been realized and experiments before and after irradiation with protons and neutrons have been performed and compared to T-CAD simulation studies with Synopsys Sentaurus. The measurements combine the electrical characteristics measured with a semi-automatic probestation with Sr90 signal measurements and analogue readout. Furthermore, some samples have been investigated with the help of a cosmic telescope with high resolution allowing charge collection studies of MIPs penetrating the sensor between two strips.

Keywords: Radiation hardness, Silicon detector, Strip isolation technology, p-stop parameter

1. Introduction

Increasing demands for more radiation hard silicon detectors for high energy physics experiments at the LHC at CERN in Geneva require detailed studies of different sensor technologies based on silicon. Several studies towards more radiation hard detectors have been carried out, with the result that the n-in-p technology is more radiation hard compared to the p-in-n type, considering the efficiency of charge collection (1; 2; 3). Therefore, more detailed studies of the n-in-p detectors have been started in order to optimize their overall performance with respect to low noise and power but simultaneously high charge collection efficiency. Several wafer submissions with different vendors to semiconductor industry have been performed. All wafer layouts included specific test structures and test sensors which should ensure the comparability of measurements and allow a comprehensive conclusion on the n-in-p type technology. One of the key interests of n-in-p type detectors is the necessary isolation layer due to the accumulation of electrons beneath the sensor surface. The attractive potential for negative charges is generated by the positive charges in the silicon dioxide which even increases with increasing fluence. Three different techniques of isolation layer have been developed, the p-spray, which is a uniform layer covering the whole wafer, p-stop which is a individual pattern for each strip or pixel, and the combination of both. However, electrical breakdown and charge collection studies indicate that the process parameters of the p-stop structure have to be carefully calibrated in order to achieve a sufficient strip isolation and high interstrip resistance, but simultaneously high breakdown voltages. Several investigations among different experiments did not allow to conclude on whether the p-spray or the p-stop tech-

nique is more suitable to ensure sufficient strip isolation after very high fluence. There are indications that the calculation of the p-spray implantation dose and energy is more challenging compared to the p-stop (4). In the study presented, the p-stop technique is investigated in detail.

2. Radiation level

During the long shutdown 3, starting at around 2024, the LHC accelerator will be upgraded to deliver higher luminosity. As a consequence the CMS Tracker has to be fully replaced in order to be compatible with the increasing radiation level and further demands, which are not discussed here. Basically, the new tracker will be composed of a pixel detector with a range of up to r < 20 cm and an Outer Tracker covering the regions 20 cm < r < 110 cm. Strip and macropixel sensors at the inner radii of the Outer Tracker will face a hadron fluence of up to 1×10^{15} $n_{eq}cm^{-2}$ after the target integrated luminosity of about 3000 fb^{-1} over 10 years of operation. As a consequence, irradiation studies have been performed with protons and neutrons with the maximum fluence of $\Phi = 2 \times 10^{15}$ $n_{eq}cm^{-2}$. The neutron irradiation took place at the TRIGA Mark II reactor in Ljubljana (5) whereas 23 MeV protons have been chosen for the irradiation with charged hadrons at the ZAG in Karlsruhe (6). The irradiations have been done in several steps covering the range from $\Phi = 1 \times 10^{14}$ $n_{eq}cm^{-2}$ to $\Phi = 2 \times 10^{15}$ $n_{eq}cm^{-2}$.

3. Silicon sensors: n-in-p technology

Figure 1 shows an image section taken from the GDS[1] file, which has been used for the sensor production. The pitch (p) of the sensors in this study is either 80 μm or 90 μm. The n+ implants for the strips are 18 μm and 20 μm resulting in a width-to-pitch ratio of 0.22 for all sensors in this study. Key properties of the isolation technique under study are the p-stop doping concentration and the p-stop pattern. The latter means the p-stop to strip implant distance (PS) of each individual p-stop implantation. The width of the p-stop is kept constant for all sensors to 6 μm. The aluminum overhang varies for the sensors between 4.5 μm and 6.5 μm. Besides these parameters, the specifications for the production were comparable. The substrate is float-zone silicon with <100> crystal orientation and a resistivity of 4 kΩcm to 10 kΩcm. The physical thickness
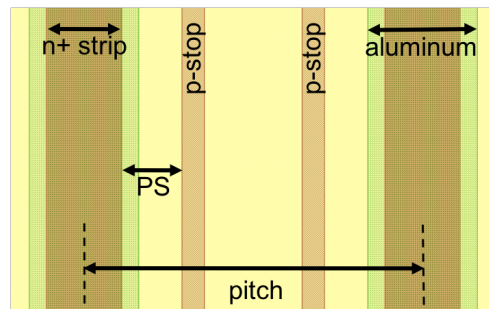

Figure 1: Scheme of two strips of a n-in-p type sensor with p-stop isolation technique extracted from a GDS file which has been used for the photolitographic masks.

Table 1: P-stop doping profile parameters of the sensors in this study.

Variant	peak conc. (cm^{-3})	doping depth (μm)	implant dose (cm^{-2})
V1	1×10^{16}	2.2	9×10^{11}
V2	9×10^{16}	2.7	8×10^{12}
V3	$<< 1 \times 10^{16}$	< 2.0	$<< 1 \times 10^{11}$
V4	1×10^{16}	1.5	7×10^{11}
V5	1×10^{16}	2.5	9×10^{11}
V6	1×10^{17}	2.5	8×10^{12}

varies for the different submissions between 200 μm and 320 μm.

P-stop characteristics

The tested strip detectors in this study mainly differ in the p-stop isolation characteristics. Sensors from four different vendors and with five different doping concentrations and doping depths have been produced and investigated. An overview of all p-stop parameters is given in Table 1. The depth is defined as the depth below the bulk surface where the doping concentration reaches the bulk concentration, (Figure 2). These values have been used for the T-CAD simulation as input parameters. The values are mainly derived from discussions with the process engineers. ToF-SIMS[2] measurements of the doping profiles are scheduled. Hereby, the composition of the surface is investigated using the sputtering of primary ions and analysis of the ejected secondary ions.

4. Experiments and simulation

The sensors have been qualified before and after irradiation. The measurements included the electrical qualification in a probestation and signal measurements with

---

[1] Graphical Design Station - data format of IC layout files

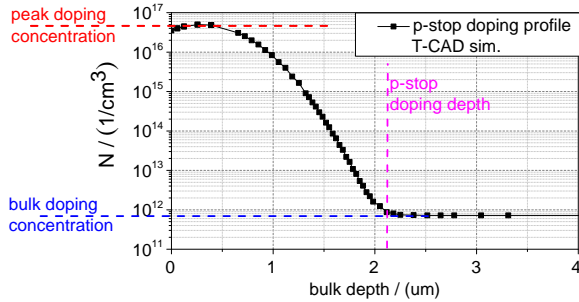[2] Time-of-Flight Secondary Ion Mass Spectroscopy

Figure 2: Exemplary doping profile used for the T-CAD simulations.

the ALiBaVa[3] (7) setup as well as T-CAD simulation studies with the Synopsys Sentaurus tool (8).

4.1. Electrical qualification

The sensors have been measured in order to investigate the isolation structure, which independent of the irradiation dose should not affect the sensor characteristics in a significant way. In particular, the breakdown voltage (V_{BD}) needs to be higher than 900V which could be reached towards the end of the sensor lifetime. As the p-stop doping concentration affects the electric field strength, the implant dose must be calculated as low as possible in order to achieve such high breakdown voltages. On the other hand, the interstrip resistance (R_{int}) requires a certain minimum of implant dose in order to ensure the minimum R_{int} of approximately 50 MΩ even after a very high fluence of $\Phi = 2 \times 10^{15}$ $n_{eq}cm^{-2}$ corresponding to an integrated luminosity of 3000 fb^{-1}. Probe needles have been used to apply the bias voltage (V_{bias}) for IV characteristics. In addition, a low voltage ramp in 0.2 V steps to 1 V between two adjacent strips has been applied. Due to the ohmic law, the R_{int} can be calculated with the measured current.

4.2. Signal measurements

The signal of the sensors has been measured with the analogue Beetle chip within the ALiBaVa setup. Calibration, clustering and signal/noise have been calculated. The analogue chip allows detailed analysis of the signal distribution and the noise behavior with and without an external source. Beta electrons from a Sr90 source have been used to generate the signal. A scintillator below the sensor provides the trigger information.

4.3. T-CAD simulation

Complementary to the measurements, T-CAD simulations with the Synopsys Sentaurus software package have been performed. The simulations have been tuned in order to reproduce the experimental data, and subsequent predictions of new sensor geometries and parameters have been investigated. As simulations of unirradiated devices can be started with the internal physics models of Sentaurus, radiation damage has to be implemented by adding additional energy levels and cross sections into the bandgap. Within a huge measurement campaign (9) of silicon sensors for the CMS Phase II Upgrade, several T-CAD damage models based on measurements have been developed, which are able to reproduce data up to a fluence of $\Phi = 1.5 \times 10^{15}$ $n_{eq}cm^{-2}$ with great agreement (10). Table 2 shows the model used in this study. This is an effective two-defect damage model for proton irradiation, the neutron model has not been used. All variants but the variant V1 have been irradiated with 23 MeV protons. V1 samples received a mixed irradiation of protons and neutrons.
From the simulations, the maximum electric field strength and the charge collection depending on the sensor parameter and fluence of the samples have been extracted.

5. Combined results from measurement and simulation

As mentioned before, the focus of this study was to find the optimum p-stop doping concentration and depth. Therefore, the samples have been electrically qualified and investigated regarding their charge collection before and after irradiation for comparison.

5.1. Electrical qualification

One of the key parameter of n-in-p type sensors is the interstrip resistance R_{int}. Measurements for all variants have been performed before and after irradiation. For comparison the R_{int} values are normalized to 1 cm strip lenght and plotted in Figure 3.

The specification of $R_{int} > 50$ MΩ mentioned in section 4.1 is valid independent of the irradiation as long as the minimal projected surface concentration is in the order of 9×10^{11} cm^{-2}. It is noticeable that the projected surface concentration of V3 with less than 1×10^{11} cm^{-2} has been chosen too low leading to values for the interstrip resistance of a few tens of kΩcm which would significantly affect the position resolution of the sensor in a negative way. The increase of the R_{int} for the low

---

[3]A Liverpool Barcelona Valencia

Table 2: Effective two-defect damage model for proton irradiation of silicon sensors for T = 253 K. E_C and E_V are the edge energies of the conduction and valence band. σ_e and σ_h are the cross sections for electrons and holes. Φ is the fluence.

Defect	Energy (eV)	σ_e (cm^{-2})	σ_h (cm^{-2})	Concentration (cm^{-3})
Acceptor	$E_C - 0.525$	1.2×10^{-14}	1.2×10^{-14}	$1.55 \times \Phi$
Donor	$E_V + 0.48$	1.2×10^{-14}	1.2×10^{-14}	$1.395 \times \Phi$
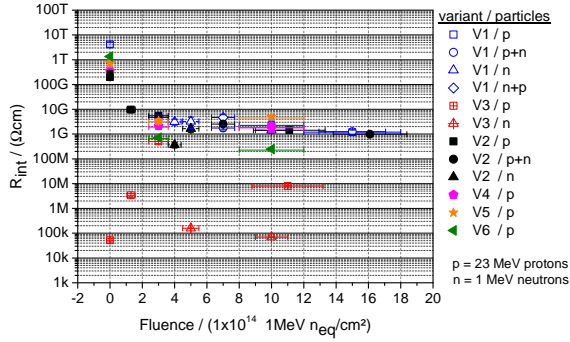
Figure 3: Interstrip resistance for the different variants as a function of the fluence.

concentration values after proton irradiation can be explained by the increase of the negative space charge towards the surface due to the ionization of acceptor traps. The resulting negative space charge repels the electrons at the surface and avoids the buildup of an accumulation layer. More detailed studies of this effect are ongoing. The variants V2 and V6 with comparably high projected surface concentration of about 8×10^{12} cm^{-2} do not show any suspicious effects considering the R_{int}. The value is sufficient and ensures independent of the fluence a sufficient interstrip isolation.

5.2. Signal measurements

After the electrical qualification, the samples have been bonded to the ALiBaVa Beetle readout chip and the noise and signal distribution generated by passing Sr90 beta electrons have been analyzed.
Generally the noise signal of silicon sensors shows gaussian behavior. Hence, a signal is detected when the noise contribution exceeds five sigma of the gaussian noise (hit interpretation if signal $\geq 5\sigma$), (Figure 4). Depending on the p-stop isolation parameter, random ghost hits are observed which are defined for pedestal runs by counting all signals with $\geq 5\sigma$ of the gaussian fit width and divided by the number of strips and recorded events. These unexpected random ghost hits have been
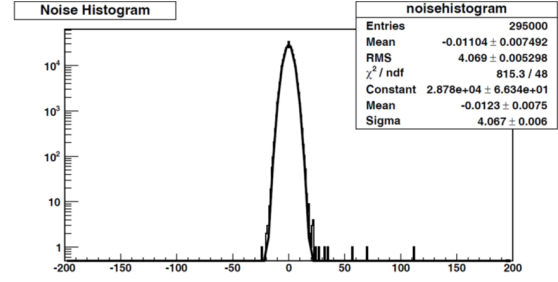
(a) Expected gaussian noise
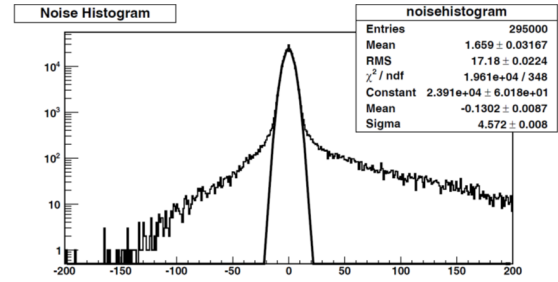
(b) Non-gaussian noise

Figure 4: Noise contribution measured in a pedestal run. The lower distribution would be interpreted as a hit by the readout electronics. This effect is observed for the variants with high p-stop doping concentrations.

observed within a huge measurement campaign for p-in-n type sensors only, in which the n-in-p type sensors have been of the variant 1 in the study presented. A random ghost hit occupancy of 1% and higher was defined as bad. The occurrence strongly depends on the fluence, the bias voltage and the particle type of the irradiation. A detailed summary on this effect is described in (11).

Random ghost hits have now also been observed in this study for n-in-p type sensors depending on the p-stop doping profile. The most probable values (MPV) of the signal during the measurements for all variants are plotted in Figure 5 as a function of the fluence without annealing and for a bias voltage of $V_{bias} = -600$V. Measurements with random ghost hits are indicated by the RGH label. It can be seen that the occurrence of RGHs is just observed for the variants V2 and V6,
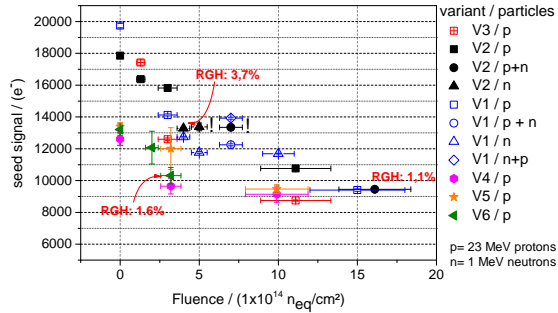
Figure 5: Signal of the different sensor variants in this study. Sensors showing RGH effects are indicated by the RGH label.

Figure 6: Section from T-CAD simulation of the V2 sample with a high p-stop doping concentration. The simulation was performed for $T = 253$ K and $V_{bias} = -600$V. The asymmetry between the p-stops is due to the chosen mesh density.

Figure 7: Maximum electric field strength distribution between two strips as a result from T-CAD simulations. The parameters correspond to the values listed in Figure 6. (The asymmetry between the p-stops is due to the choice of the mesh parameter.)

which have a comparably high p-stop doping concentration of about 1×10^{17} cm^{-3}. High random ghost hit rate (>1%) is observed already at relatively low fluence of $\Phi = 4 \times 10^{14}$ n$_{eq}$cm^{-2} for neutron irradiation. This can be explained by taking the surface damage into account. Damage of the silicon dioxide at the sensor surface is introduced less by neutrons compared to protons which deposit energy by ionization. As a consequence, the positive charge of the silicon dioxide does not increase significantly, leading to higher peak electric field strength in the bulk compared to proton irradiated samples (11).

T-CAD studies indicate that the electric field strength can even exceed 3×10^5 Vcm^{-1}, which is the breakdown voltage of a pn junction in silicon. A section from the T-CAD simulation of sample V2 in Figure 6 shows high electric fields occurring directly at the p-stop edges and exceeding 3×10^5 Vcm^{-1}. The values for the electric field have been extracted 0.5 μm beneath the surface and plotted as a function of the position between the strips in Figure 7. With this observation, the RGH rate in n-in-p type samples can now be explained.

The physics model for the avalanche effect starts to generate charges for electric fields in the range between 1.75×10^5 Vcm^{-1} and 6×10^5 Vcm^{-1} (blue line in Figure 7) after the van Overstraetende Man model (12). These avalanche electrons are then detected with the readout electronics and wrongly interpreted as charges generated by ionizing energy loss from traversing particles. Simultaneously, simulations of variants V1, V3, V4 and V5 with moderate p-stop doping concentrations do not indicate a generation of avalanche electrons at all due to lower maximum electric field strengths.

Furthermore no significant effect of the p-stop doping depth has been observed, neither in the electrical qualification nor in the ALiBaVa measurement. Hence, con-
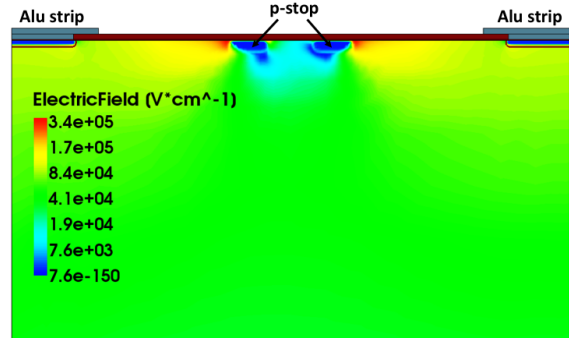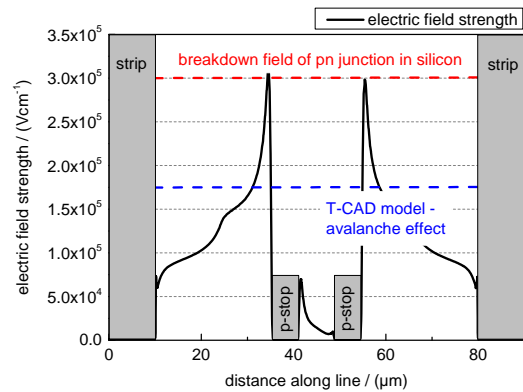
sidering the experimental data, no clear recommendation on the p-stop depth can be expressed whereas a peak p-stop doping concentration of 1×10^{16} cm^{-3} seems to be sufficient with respect to good microstrip isolation and breakdown voltage. Also the charge collection efficiency (CCE) seems to be independent of the p-stop process characteristics. For a more detailed CCE study, the samples have to be measured during test beam conditions with a telescope in order to achieve a substrip resolution of the hits.

The successful reproduction by simulation of experimental data has been proven in (10) and (13). Therefore, the model in Table2 has been used for a scan of the electric field strength in a sensor as a function of the
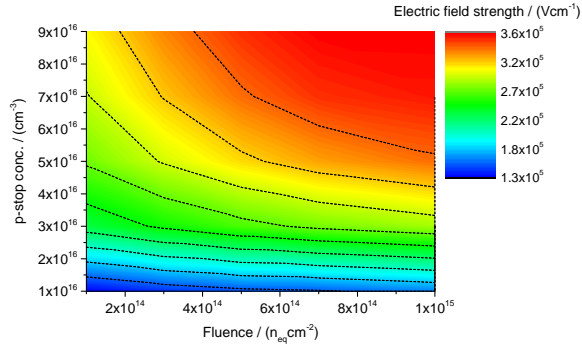
Figure 8: Maximum electric field strength in the bulk of a silicon strip sensor in dependence on the p-stop doping concentration and proton fluence. Simulation has been performed for T = 253 K and $V_{bias} = -600$ V.

Figure 9: Comparison of signal for sensors with different PS values from measurements and T-CAD prediction.

Figure 10: Electric field 0.5 μm below the sensor surface for two different PS values in the unirradiated case.

fluence and the p-stop doping concentration. The result is shown in Figure 8. The outcome is very well comparable to the measurements, meaning that the expected high electric field strengths of 1.75×10^5 Vcm^{-1} and higher are reached when the p-stop doping concentration reaches at least the minimum of $2 - 3 \times 10^{16}$ cm^{-3}. The doping depth for the numerical analysis was constantly 2 μm and comparable to the depth of the variants in this study. Combining results from the electrical qualification, signal measurements and T-CAD studies, the doping concentration of 1×10^{16} cm^{-3} and a doping depth of around 2 μm seems to be the most appropriate considering the strip isolation and low random ghost hit rate, respectively low electric field strengths.

The same procedure has been performed for a fixed p-stop doping concentration but varying the p-stop to strip implant distance (PS), (Figure1). The maximum electric field strengths in the bulk have been extracted from simulations with constant sensor geometry and parameters but the PS.

Considering the signal, no indications on optimal PS values are given for both measurement and simulation, Figure 9. On the other hand, Figure 10 shows slightly higher electric fields when the p-stop is close to the strip n+ implant. In this case, the electric field is more concentrated between p-stop and strip in comparison to a wider distance between the two implants. This is especially of interest for the photolithographic mask designers who with a wide PS do not have to design special and complex routing of the p-stop around the sensor AC pads.
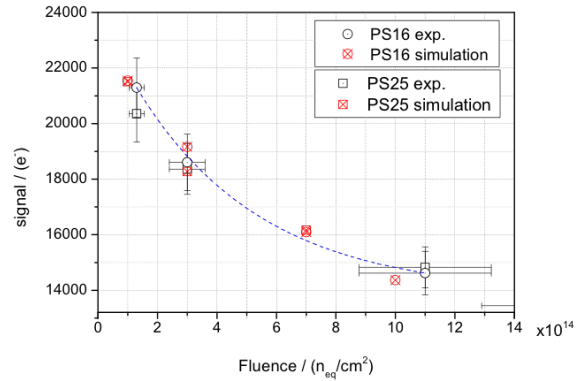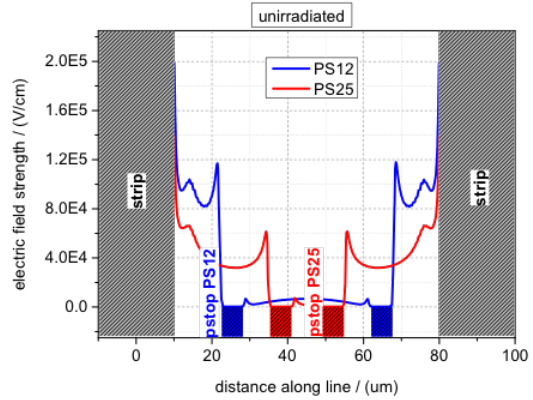
6. Conclusion

The future CMS silicon outer tracker will use n-in-p type sensors. Critical detector parameters like the pitch and strip implant width and concentration are fixed and do not need any further investigations towards radiation hard silicon sensors for HL-LHC lifetime. The necessary strip isolation by implantation of group III elements, however, needs to be carefully calculated in order to ensure a sufficient interstrip isolation without negative impacts on the sensor performance.

In this study, sensors with different p-stop isolation parameters have been investigated for their radiation hardness in dependence on the p-stop doping concentration and depth. Interestingly, no significant differences of the variants in the electrical qualification have been observed, whereas undesired random ghost hits occurred after irradiation for high p-stop doping concentrations.

The combination of data and T-CAD studies clearly prefers doping concentrations of around 1×10^{16} cm^{-3}, while the p-stop doping depth does not show significant influence. The distance between the floating p-stop and grounded strip implants is favored to be wide, or rather the p-stop implants should be placed in the center between adjacent strips. Further studies, especially beam tests with substrip resolution, are scheduled.

7. Acknowledgement

[1] A. Junkes. Planar silicon sensors for the CMS tracker upgrade. *Nucl. Instr. and Meth. A*, 732:113–116, 2013.

[2] A. Dierlamm. Planar sensors for future vertex and tracking detectors. *PoS(Vertex 2013)*, 027, 2013.

[3] A. Nuernberg. *Studies on irradiated silicon sensors for the CMS tracker at the HL-LHC*. PhD thesis, KIT, 2014.

[4] C. Fleta et al. P-spray implant optimization for the fabrication of n-in-p type microstrip detectors. *Nucl. Instr. and Meth. A*, 573, 2007.

[5] TRIGA Mark II. www.rcp.ijs.si/ric/description-a.html, November 2015.

[6] Zyklotron AG. http://www.zyklotron-ag.de, November 2015.

[7] R. Marco-Hernandez. A portable readout system for silicon microstrip detectors. *Nucl. Instr. and Meth. A*, 623:207–209, 2010.

[8] Synopsys Sentaurus T-CAD, October 2015.

[9] K.-H. Hoffmann. Campaign to idetify the future CMS tracker baseline. *Nucl. Instr. and Meth. A*, 658:30–35, 2011.

[10] Robert Eber. *Investigations of new Sensor Designs and Development of an effective Radiation Damage Model for the Simulation of highly irradiated Silicon Particle Detectors*. PhD thesis, KIT, 2013.

[11] Martin Printz. Radiation Hard Sensor Materials for the CMS Tracker Phase II Upgrade - Charge Collection of Different Bulk Polarities. *Nucl. Instr. and Meth. A*, 2014.

[12] R. van Overstraeten and H. de Man. Measurement of the Ionization Rates in Diffused Silicon p-n Junctions. *Solid-States Electronics*, 13(1):583–608, 1970.

[13] Martin Printz. T-CAD analysis of electric fields in n-in-p silicon strip detectors in dependence on the p-stop pattern and doping concentration. *JINST*, 10(C01048), 2015.